Modeling stand-level forest attributes using lidar and Common Stand Exam data

Brett L Lawrence [AB] *

[A] Stephen F. Austin State University, 1936 North St, Nacogdoches, Texas 75962, USA

[B] Raven Environmental Services, Inc., 6 Oak Bend Drive, Huntsville, Texas 77340, USA

*Corresponding Author: +1-936-581-6833, lawrenceb3@jacks.sfasu.edu;

This manuscript a non-peer reviewed preprint submitted to EarthArXiv. It has also been submitted to scientific journal, and following peer-review will potentially undergo changes from its preprint version.

Abstract

This study focuses on the development of a lidar-based methodology that recreates stand-level inventory results from Common Stand Exams (CSE). CSE protocols are the U.S. Forest Service's approach to measuring forest stocking and volume on public lands. Using an open-sourced dataset, stand-level statistics of lidar-derived height metrics, individual tree height, and tree density were generated for 105 stands on the Sam Houston National Forest in Montgomery County, Texas, US. When comparing traditionally acquired CSE data versus lidar-based analysis, we successfully modelled linear relationship of stand-level pine basal area (BA) ($R^2 = 0.41$), trees per acre (TPA) of pine ($R^2 = 0.61$), and pine volume ($R^2 = 0.58$). Similar studies often compare lidar-based metrics to individual plot results, whereas our workflow demonstrated reasonable extraction of stand-level metrics from an established forestry protocol. While lidar-based approaches might not be appropriate for every forest management objective, our results demonstrate that they have the potential to be leveraged in scenarios where relatively coarse results are acceptable. Where open-sourced data is available, this could represent significant time and cost efficiency for forest managers who are confronted with challenging deadlines, fiscal limitations, and harsh environmental conditions.

Keywords: lidar, Common Stand Exam, shortleaf pine, loblolly pine, forest inventory

Introduction

Stand-level forest inventory data is an important resource for managers making decisions about forest prescriptions and treatments. Forest management often happens at the stand-level or multi stand-level scale but stand inventory and volume data are not always readily available. Its acquisition can be

cost-prohibitive and time-prohibitive, with timber cruises requiring significant personnel time in the field.

Alternatives that reduce or eliminate the need for personnel intensive field work have been applied using a variety of methods (Hummel et al., 2011; Brosofske et al., 2014; Hemingway and Opalach, 2024). They typically involve the acquisition of some remote sensing dataset using spaceborne, airborne, or UAV-borne methods, and analyzing that data to model forest attributes. When and where these methods can be applied effectively is highly circumstantial, and depend on factors such as resource availability, budget, and the spatial scale being assessed. For example, a UAV or drone might be a cost-effective option for forest managers with limited resources and budget, but the spatial scale they operate within is relatively small and inadequate for assessing larger areas.

Lidar is often the foundational remote sensing dataset used when recreating forest attributes that characterize structure (Dubayah et al., 2000; Balestra et al., 2024). Lidar data is comprised of laser pulses from the sensor, or returns, that measure the heights of vegetation and physical features on some terrestrial surface. The resulting point cloud datasets are capable of modeling forest vegetation in precise detail (Sumnall et al., 2021; Ross et al., 2024). Examples include modeling tree height, canopy size, tree density, or even characteristics such as species richness and composition (Anderson et al., 2021; Wu et al., 2024).

Frequently, estimates of forest structure using lidar data are validated with plot-level field inventories (Means et al., 2000; Woods et al., 2008). It was our goal to quantify lidar inventory metrics at the stand level and compare them to results of an established inventory protocol called Common Stand Exams (CSE). CSEs are agency-specific forest inventory method used by the U.S. Forest Service. Also, we sought to do so with an open-source lidar dataset that would allow us to avoid the cost of acquiring project-specific data. For this study, a 2018 USGS airborne lidar dataset was collected two years prior to a traditional forest inventory conducted on the Sam Houston National Forest in Walker

County, Texas, United States. We used this dataset to determine whether a geoprocessing workflow could be developed for recreating stand-level volume, basal area (BA), and trees per acre (TPA) from our CSE forest inventory.

Methods

2.1 Study area

CSE data was collected in 105 stands within compartments 31-33 on the Sam Houston National Forest (SHNF) in Spring 2020 (Figure 1). The SHNF is located in Walker, Montgomery, and San Jacinto counties of Texas, United States, and is often characterized by mixed loblolly pine and shortleaf pine overstory. The two can vary in their presence and abundance, with shortleaf pine being an upland species and loblolly pine being a ubiquitous species. Major hardwood species include southern red oak (*Quercus falcata*), post oak (*Quercus stellata*), cherrybark oak (*Quercus pagoda*), American sweetgum (*Liquidambar styraciflua*), black tupelo (*Nyssa sylvatica*), and winged elm (*Ulmus alata*). Hardwoods generally represent a small percentage of stand species composition (<15%), with some exceptions on the east, northeast sides of the study site. Soils are mostly characterized by fine sandy loams and loamy fine sands, with some areas of eroded and frequently flooded clay soils to the northeast of the site.

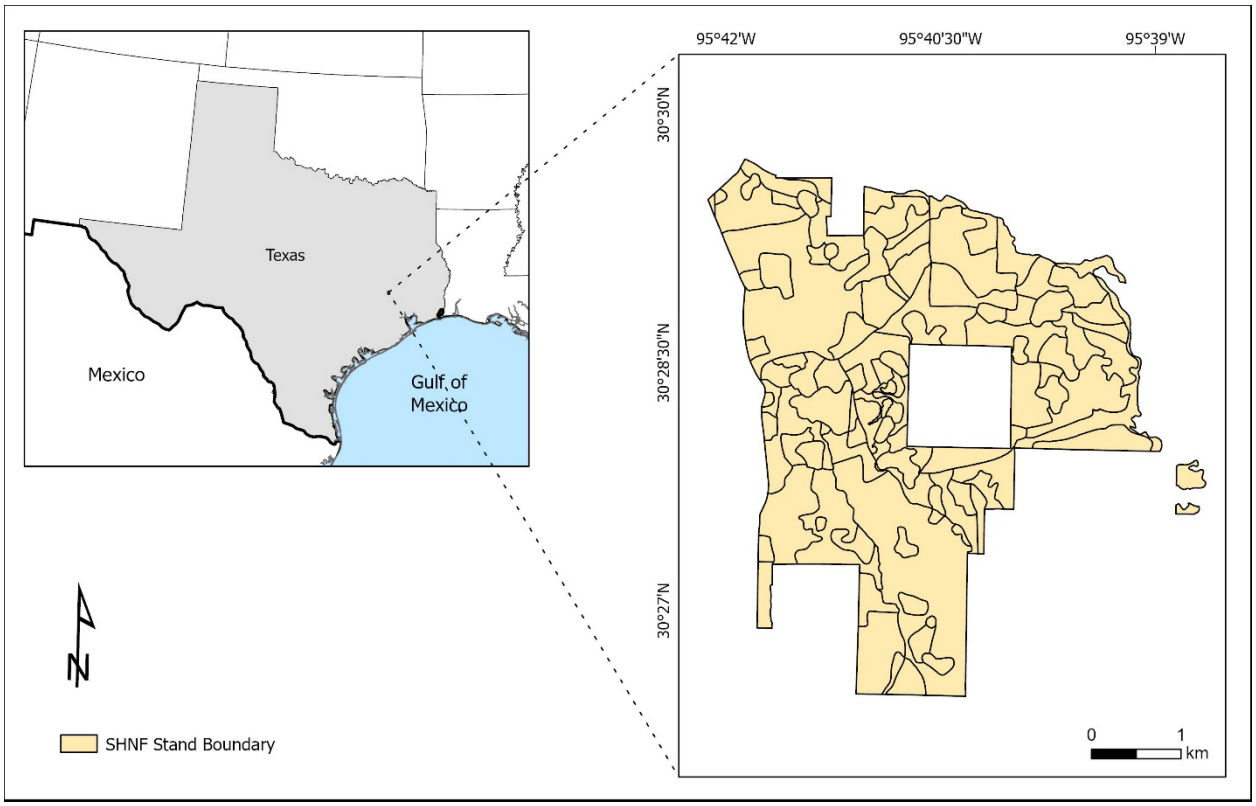

Fig. 1. Stands within Compartments 31-33 on the Sam Houston National Forest in Montgomery County, Texas, United States. CSE data collected on the site in Spring of 2020.

2.2 Workflow

The workflow is broken into three major steps that consisted of creating independent variables from lidar data, conducting an correlation analysis to filter independent variables, and using a small selection of them to model linear relationships with dependent variables or CSE data (Figure 2). The Upper Coast Lidar (UCL) dataset was used for our analysis and sourced from the Texas Natural Resources Information System website (Texas Natural Resource Information System, 2018). Lidar data was collected on January 13th, 2018 through March 22nd, 2018 during leaf-off conditions, with our study area using 11 of 9,758 tiles that comprise the entire UCL dataset. UCL data was acquired using a manned aircraft at a nominal point density of 4.37 pts/m^2 (Texas Water Development Board, 2018). Riegl LMS-Q680i and Riegl LMS-Q780 sensors were used at a flight altitude of

approximately 780 m and a measurement range of 1 to 2 km. A significant portion of analyses in this study were conducted using the lidR package in R Studio (R version 2024.04.2+764) (Roussel et al., 2020) and ArcGIS Pro software (ESRI, Redlands, California, U.S.).

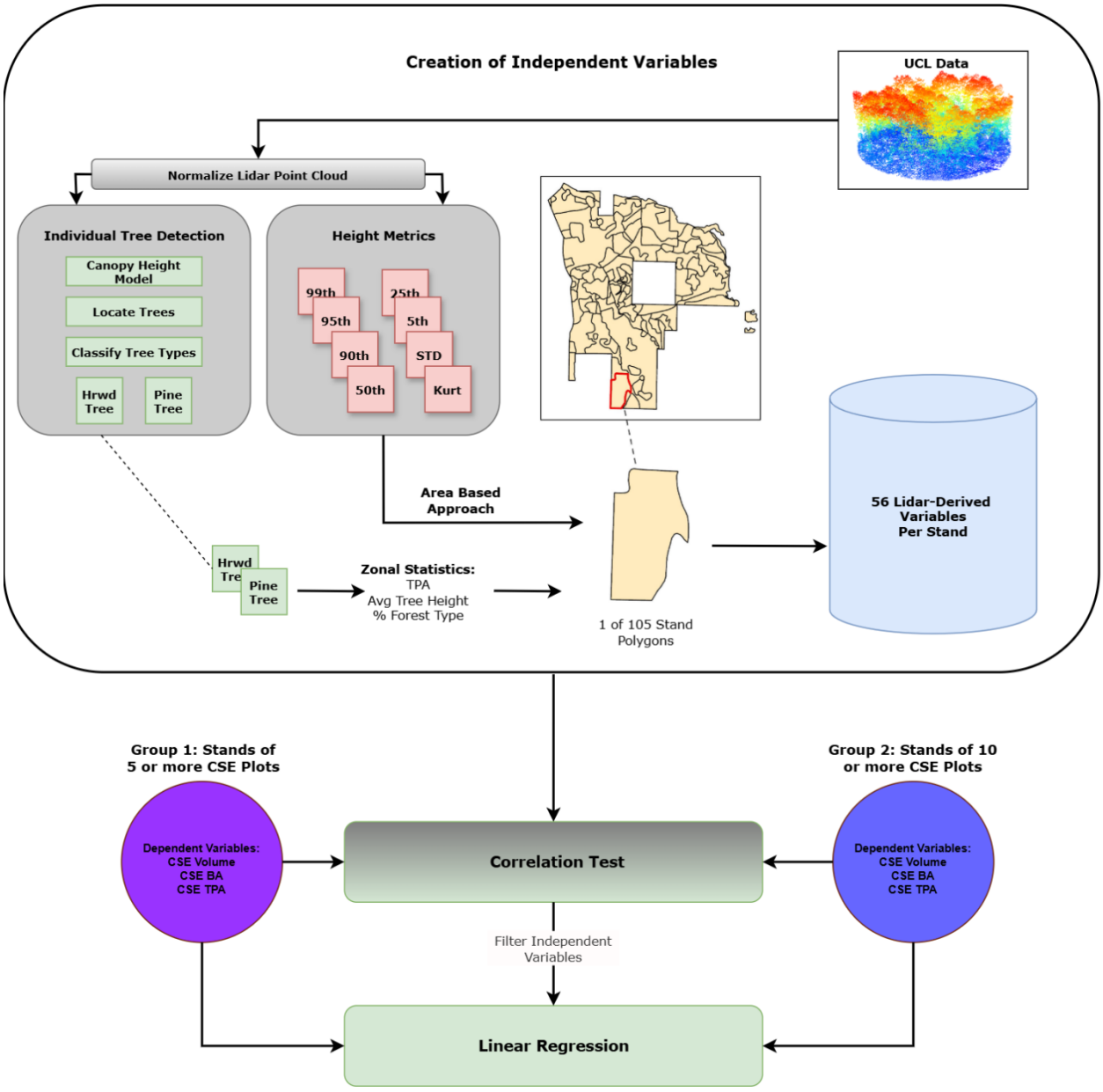

Fig. 2. A workflow of how lidar data was used to generate height metrics and individual tree detections. These were then used to generate zonal statistics for each stand in the study area. The resulting independent variables were filtered using a correlation analysis, and a small selection of them were used in a regression analysis with CSE inventory data (dependent variables).

2.2.1 Generating Lidar-derived Independent Variables

To support the evaluation of stand-level forest attributes, a total of 36 height metrics were generated for each stand (Table 1). Before generating height metrics, a catalog of tiled lidar files was created and normalized. An area-based approach was then used to generate metrics for regions of interest (ROIs) within the normalized point cloud. Our ROIs were created using a shapefile of 105 stands in the study area (Figure 2). Each stand was clipped from the point cloud, and lidar height metrics calculated for that respective stand.

Table 1. A summary of all lidar-derived independent variables (56 total) and CSE dependent variables used for analysis (12 total).

Variable Group	Number of Variables	Variable Names	Description
Lidar-derived Independent Variables: 56 Total			
Height Metrics	36	zmax, zmean, zsd, zskew, zkurt, zentropy, pzabovezmean, pzabove2, zq5, zq10, zq15, zq20, zq25, zq30, zq35, zq40, zq45, zq50, zq55, zq60, zq65, zq70, zq75, zq80, zq85, zq90, zq95, zpcum1, zpcum2, zpcum3, zpcum4, zpcum5, zpcum6, zpcum7, zpcum8, zpcum9	All height values created using lidr plot metrics and calculated for each stand using an area-based approach.
Individual Tree Detection – All	8	all_mean_z, all_std_Z, all_max_Z, all_min_Z	Average, minimum, maximum and standard deviation of stand-level heights (hardwood and pine).
		tree_count, all_TPA	Total trees and TPA at the stand-level (hardwood and pine).
		minority_forest_class_ercent, majority_forest_class_percent	Percentage of forest class for each stand, either hardwood or pine.
Individual Tree Detection - Pine	6	pine_mean_z, pine_std_Z, pine_max_Z, pine_min_Z	Average, minimum, maximum and standard deviation of stand-level heights (pine only).
		pine_count, pine_TPA	Total trees and TPA at the stand-level (pine only).
Individual Tree Detection - Hardwood	6	hrwd_mean_z, hrwd_std_Z, hrwd_max_Z, hrwd_min_Z	Average, minimum, maximum and standard deviation of stand-level heights (hardwood only).
		hrwd_count, hrwd_TPA	Total trees and TPA at the stand-level (hardwood only).
Dependent Variables: 12 Total			
Stand-level CSE Metrics	9	total_BA, pine_BA, hrwd_BA, total_TPA, pine_TPA, hrwd_TPA, pine_cubic, pine_merch, pine_board	Traditional, ground-based inventory metrics.

Besides the stand-level height metrics, individual tree detection was also performed within the study area. The cataloged and normalized lidar point cloud was first rasterized into a canopy height model (CHM). We used a pit free algorithm known for improving tree detection (Khosravipour et al., 2014), and post-processed the CHM using smoothing and filling. Trees were detected using a local maximum filter approach and a constant window size of 5 m. The resulting tree points and corresponding heights were exported to a shapefile format.

To identify which points belonged to major forest classes of pine or hardwood, we generated a classified raster of both forest types using supervised classification of imagery captured by the National Agricultural Imagery Program (NAIP) (USDA, n.d.). NAIP imagery was made up of 60 cm resolution RGB and near-infrared bands and was collected the same year as our UCL lidar dataset (December 2018). A simple class schema of "pine", "hardwood", and "other" was used to classify pixels. Once a classification raster was created, each tree detection point was assigned a forest class based on the pixel type it spatially coincided with. Zonal statistics were then calculated that considered the total number of trees, TPA, average tree height, maximum tree height, and minimum tree height per stand. These metrics were individually generated for all trees, pine trees, and hardwood trees. A total of 20 individual tree detection metrics were generated and used as lidar-derived independent variables (Table 1).

2.2.2 Common Stand Exam Data: Statistical Groups and Analysis

CSE inventory data was collected from March 2020 to June 2020 using protocols detailed in the U.S. Forest Service's Region 8 Common Stand Exam Field Guide (Region 8 – Common Stand Exam, n.d.). While there was an approximately 2-year difference in lidar data capture and the CSE field inventory, our study area had not undergone any noteworthy changes in structure from natural forces (i.e. drought, hurricane) or management practices (i.e. timber harvest, vegetation management) during this time. Large temporal misalignment in lidar validated inventories can lead to decreased

model performance but have been shown to be less impactful in situations like ours where gaps are four years or less (Babcock et al., 2016).

CSE stand level metrics, or dependent variables, included: total BA, pine BA, hardwood BA, pine TPA, hardwood TPA, board ft volume of pine, merchantable volume of pine, and cubic volume of pine. The original 105 stands were filtered into two statistical groups: the first included stands where 5 or more CSE plots were collected (43 of 105 stands), and the second where 10 or more CSE plots were collected (16 of 105 stands). This allowed the analysis to focus on stands where sufficient field data was gathered. Prior to performing any linear regression analysis, a Pearson's correlation was calculated to assess relationships between all variables and filter out non-significant ones. The "metan" package in R was used to expedite this process, and narrow down examples of statistically significant relationships between independent and dependent variables, and the strength of their correlation. For both statistical groups, linear regression was performed at a 95^{th} confidence interval using dependent and independent variables with the strongest correlation. Using the "rempsyc" package in R, we tested all models for assumptions of normality, heteroscedasticity, and autocorrelation of residuals. Any models violating the assumptions necessary for linear modeling were excluded from our results.

Results and Discussion

3.1 Linear Regression: 1st Group

When analyzing CSE stands that were comprised of 5 plots or more (n = 43), we identified numerous examples of lidar-derived variables and CSE metrics with statistically significant relationships. Amongst these, a smaller number met the assumptions of linear regression, of which we have shared the best performing models (Figure 3). Total BA and pine BA were both significantly predicted (P <

0.001) by estimates of pine TPA created from individual tree detection ("lrd_pine_TPA"), with models explaining 31% and 41% of the variance, respectively. The lidar-derived height metric "zq55" significantly predicted ($P < 0.001$) hardwood BA and explained 22% of the variance. Pine board volume, pine cubic volume, and pine merchantable volume were all significantly predicted ($P < 0.001$) by both individual tree and height metrics, with 32-41% of the variance explained. When analyzing this group, we did not successfully model pine or hardwood TPA with any lidar-derived variables.

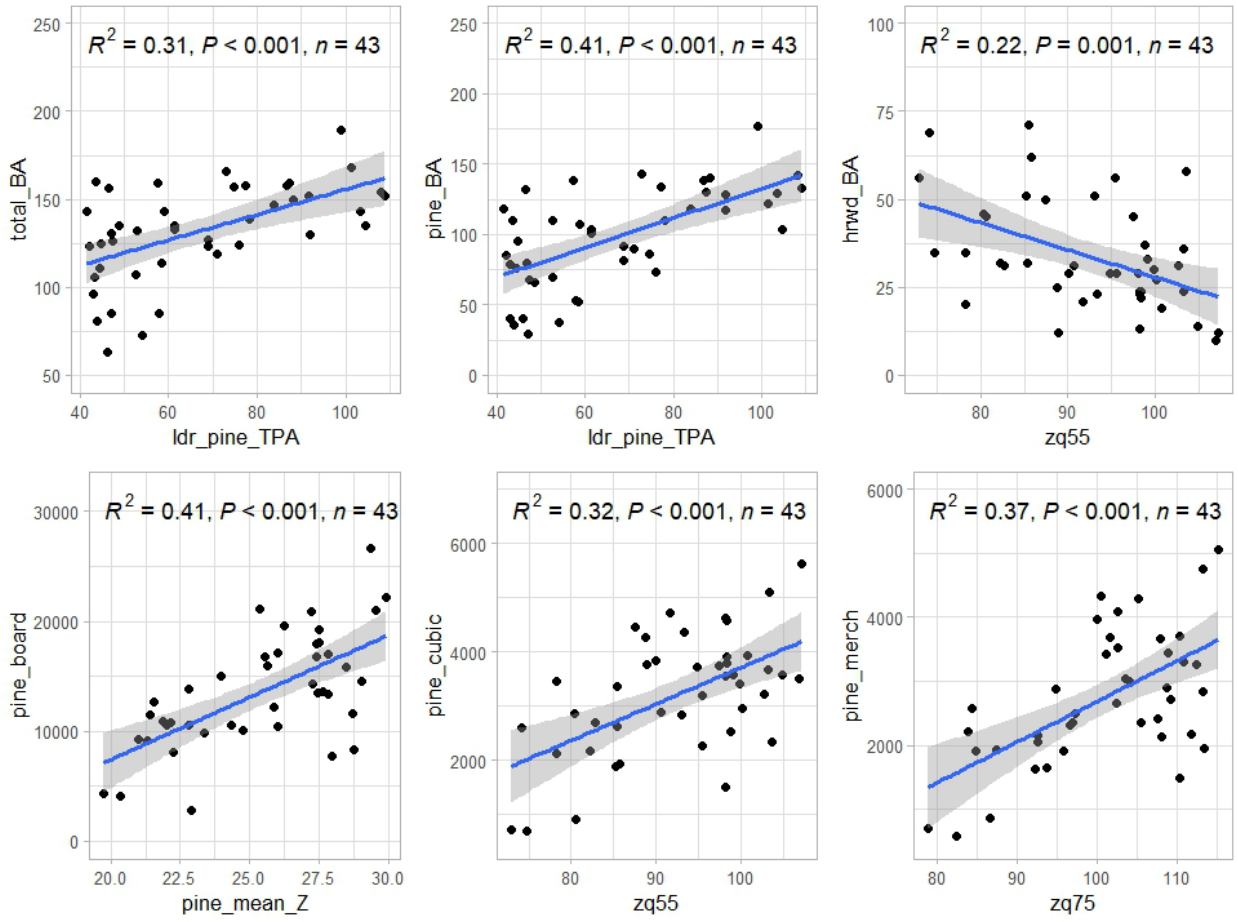

166 **Fig. 3.** Results of linear regression when modeling CSE metrics and lidar-derived variables in stands
167 where 5 or more CSE plots were collected.

168 ***3.2 Linear Regression: 2nd Group***

169 For CSE stands with 10 or more plots (n = 16), lidar metrics generated from individual tree detection
170 consistently produced the highest performing models, with one exception. Both total BA (P = 0.008)
171 and pine BA (P = 0.009) were significantly predicted by lidar measurements of all TPA
172 ("ldr_all_TPA"), with linear regression explaining 41% and 40% of the variance, respectively. Lidar
173 measurements of average tree height per stand ("all_mean_Z") significantly predicted pine TPA (P <
174 0.001) and pine board ft. volume (P < 0.001). For those models, lines of best fit explained 61% of the
175 variance for pine TPA and 58% for board ft. volume. Volume of merchantable pine was
176 significantly predicted (P = 0.002) by the lidar height metric "zq75", with 51% of the variance
177 explained.

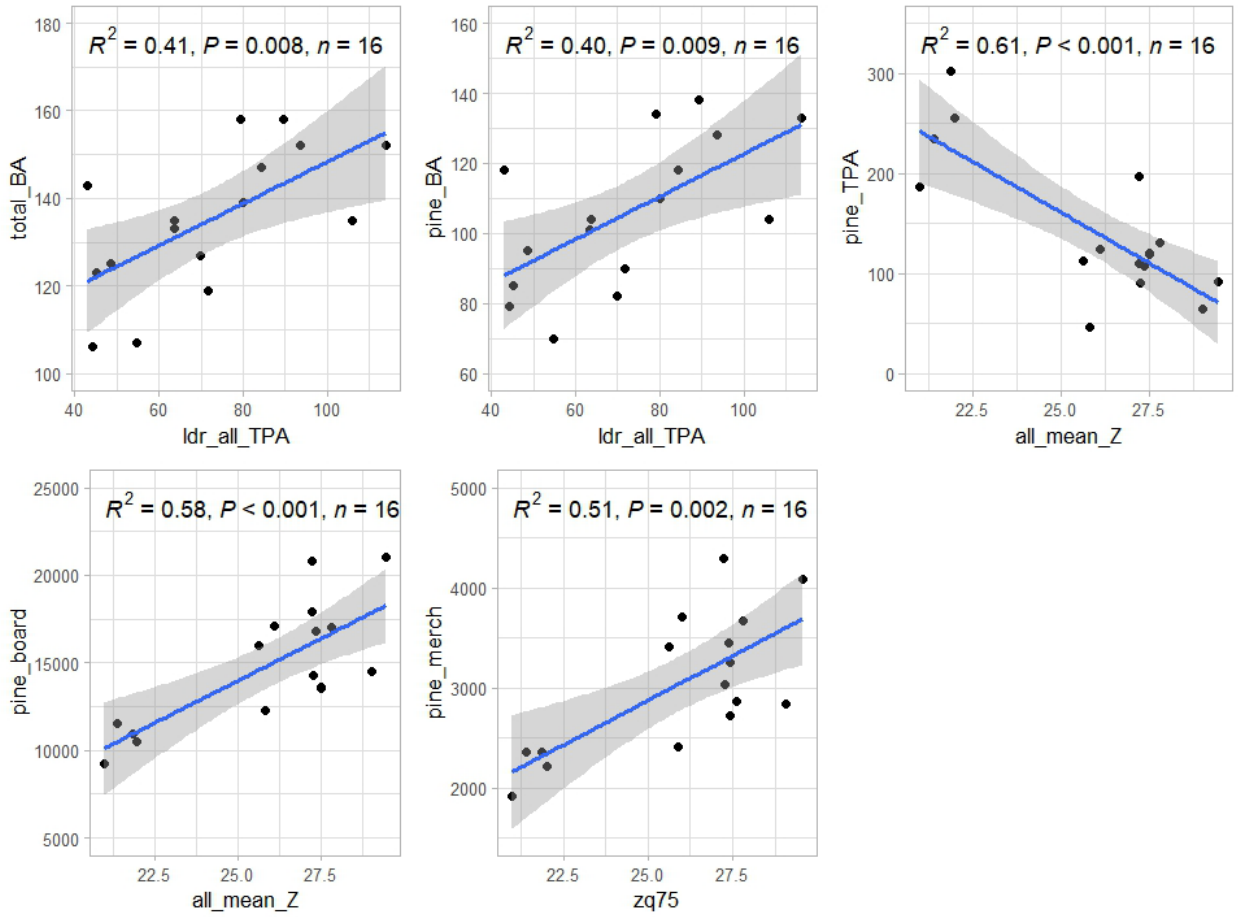

Fig. 4. Results of linear regression when modeling CSE metrics and lidar-derived variables in stands where 10 or more CSE plots were collected.

3.3 Lidar and Stand-level Inventories

The results of our analysis indicate that open sourced lidar can be processed into explanatory variables used for modelling predictions of traditionally collected CSE data. This was true of lidar-derived metrics from individual tree detection and height metrics, with both being statistically significant predictors of a variety of CSE dependent variables. Amongst our 9 dependent variables, we were able to successfully create predictive linear models for all but hardwood TPA and TPA for all forest types. Of the numerous studies published exploring the use of lidar to generate forest attributes, we only identified one that focused on the U.S. Forest Service's CSE protocol (Hummel et

al., 2011). In their study, they had limited success modeling CSE stand volume, whereas our analysis successfully modelled volume in CSE stands of 5 or more plots, and 10 or more plots.

Whether our methods could be practically applied in a real-world setting is arguably circumstantial. For example, we excluded stands comprised of very small amounts of plots from our analysis (<5 plots). Additionally, several of our models explained a small amount of the variance (<50%) and therefore have arguably limited predictive capabilities. In some scenarios, however, it is plausible that our methods could be used for generating coarse estimates of forest structure at the stand level. Based on our results for CSE stands of 10 plots or more, modeling predictions of pine structure could be reasonably achievable. As the U.S. Forest Service is confronted with directives to increase timber production, our proposed methods could be one approach to generating estimates of stand-level structure in similar southern pine stands (USDA, 2025).

Efforts were made to improve our results by analyzing our data with machine learning models, such as random forest and best subset regression. We consistently encountered comparable, or even reduced model performance. We speculate this could be attributable to multicollinearity amongst several of our predictor variables. This was especially true of our lidar height metrics. In future work, we would consider expanded methods, like data fusion (Popescu and Wynne, 2004; Lawrence, 2024) and deep learning modelling (Mäyrä et al., 2021; Klauberg et al., 2023) to improve our analysis. Data fusion of lidar with non-visible spectra, like in Landsat or Sentinel satellite missions, is one avenue for potentially increasing the predictive powers of our analysis. Non-visible spectra have been applied previously to classify canopy coverage of southern yellow pine (Akumu and Amadi, 2022). In other examples, hyperspectral data was used to investigate whether spectral characteristics specific to each southern yellow pine species could be distinguished using field-based (van Aardt, 2000) and remote sensing methods (Van Aardt and Wynn, 2007).

Conclusion

The U.S. Forest Service owns 193 million acres of public land, and despite having an agency-specific forest inventory method, there are limited examples of lidar-derived inventories being applied to the Common Stand Exam protocol. Our study demonstrates that open-sourced lidar data is a potential means for recreating CSE metrics in certain scenarios. Most notably, in situations where CSE stands were comprised of 10 or more inventory plots, lidar-derived metrics explained moderate amounts of variance when predicting stand-level pine (BA) ($R^2 = 0.41$), trees per acre (TPA) of pine ($R^2 = 0.61$), and pine volume ($R^2 = 0.58$). This could translate to cost reductions and efficiencies, in the event traditional, personnel-intensive forest inventories could be augmented or replaced by remote sensing methods. Refinements of methodology, in particular fusing our lidar raster data with non-visible spectral data, could be one approach to modeling more accurate relationships with other CSE metrics like BA, TPA.

Declarations

Ethics approval and consent to participate: Not applicable

Consent for publication: Not applicable

Availability of data and material:

Competing interests: The authors declare that they have no competing interests.

Funding: This research received no external funding.

Authors' contributions: BL: conceptualization, data curation, formal analysis, methodology, validation, writing - original draft, and writing - review and editing.

Acknowledgements: Thank you to Dr. Ying Lu of Stephen F. Austin State University for your helpful commentary and assistance with improving the manuscript. The author thanks Kerry Hogg of the U.S. Forest Service for providing stocking and volume reports of the site and permitting the use of the data for the study. We also want to thank the Sam Houston National Forest staff for the opportunity to use the forest as a study site.

References

1. Akumu, C.E., Amadi, E.O., 2022. Examining the Integration of Landsat Operational Land Imager with Sentinel-1 and Vegetation Indices in Mapping Southern Yellow Pines (Loblolly, Shortleaf, and Virginia Pines). photogramm eng remote sensing 88, 29–38. https://doi.org/10.14358/PERS.21-00024R2
2. Anderson, C.T., Dietz, S.L., Pokswinski, S.M., Jenkins, A.M., Kaeser, M.J., Hiers, J.K., Pelc, B.D., 2021. Traditional field metrics and terrestrial LiDAR predict plant richness in southern pine forests. Forest Ecology and Management 491, 119118. https://doi.org/10.1016/j.foreco.2021.119118
3. Babcock, C., Finley, A.O., Cook, B.D., Weiskittel, A., Woodall, C.W., 2016. Modeling forest biomass and growth: Coupling long-term inventory and LiDAR data. Remote Sensing of Environment 182, 1–12. https://doi.org/10.1016/j.rse.2016.04.014
4. Balestra, M., Marselis, S., Sankey, T.T., Cabo, C., Liang, X., Mokroš, M., Peng, X., Singh, A., Stereńczak, K., Vega, C., Vincent, G., Hollaus, M., 2024. LiDAR Data Fusion to Improve Forest Attribute Estimates: A Review. Curr. For. Rep. 10, 281–297. https://doi.org/10.1007/s40725-024-00223-7

5. Brosofske, K.D., Froese, R.E., Falkowski, M.J., Banskota, A., 2014. A Review of Methods for Mapping and Prediction of Inventory Attributes for Operational Forest Management. Forest Science 60, 733–756. https://doi.org/10.5849/forsci.12-134
6. Dubayah, R., Drake, J., 2000. Lidar Remote Sensing for Forestry. Journal of Forestry 98, 44–46. https://doi.org/10.1093/jof/98.6.44
7. Hemingway, H., Opalach, D., 2024. Integrating Lidar Canopy Height Models with Satellite-Assisted Inventory Methods: A Comparison of Inventory Estimates. Forest Science 70, 2–13. https://doi.org/10.1093/forsci/fxad047
8. Hummel, S., Hudak, A.T., Uebler, E.H., Falkowski, M.J., Megown, K.A., 2011. A Comparison of Accuracy and Cost of LiDAR versus Stand Exam Data for Landscape Management on the Malheur National Forest. Journal of Forestry 109, 267–273. https://doi.org/10.1093/jof/109.5.267
9. Khosravipour, A., Skidmore, A.K., Isenburg, M., Wang, T., Hussin, Y.A., 2014. Generating Pit-free Canopy Height Models from Airborne Lidar. photogramm eng remote sensing 80, 863–872. https://doi.org/10.14358/PERS.80.9.863
10. Klauberg, C., Vogel, J., Dalagnol, R., Ferreira, M.P., Hamamura, C., Broadbent, E., Silva, C.A., 2023. Post-Hurricane Damage Severity Classification at the Individual Tree Level Using Terrestrial Laser Scanning and Deep Learning. Remote Sensing 15, 1165. https://doi.org/10.3390/rs15041165
11. Lawrence, B., 2024. Lidar-based MaxEnt models to support conservation planning for endangered Red-cockaded Woodpeckers in urbanizing environments. Remote Sensing Applications: Society and Environment 34, 101190. https://doi.org/10.1016/j.rsase.2024.101190
12. Mäyrä, J., Keski-Saari, S., Kivinen, S., Tanhuanpää, T., Hurskainen, P., Kullberg, P., Poikolainen, L., Viinikka, A., Tuominen, S., Kumpula, T., Vihervaara, P., 2021. Tree species

267 classification from airborne hyperspectral and LiDAR data using 3D convolutional neural
268 networks. Remote Sensing of Environment 256, 112322.
269 https://doi.org/10.1016/j.rse.2021.112322
270 13. Means, J.E., Acker, S.A., Fitt, B.J., Renslow, M., Emerson, L., Hendrix, C.J., 2000.
271 Predicting Forest Stand Characteristics with Airborne Scanning Lidar. Photogrammetric
272 Engineering & Remote Sensing 66, 1367–1371.
273 14. Popescu, S.C., Wynne, R.H., 2004. Seeing the Trees in the Forest: Using Lidar and
274 Multispectral Data Fusion with Local Filtering and Variable Window Size for Estimating
275 Tree Height. photogramm eng remote sensing 70, 589–604.
276 https://doi.org/10.14358/PERS.70.5.589
277 15. Region 8 - Common Stand Exam Field Guide (Field Guide), n.d. . Natural Resource Manager
278 Field Sampled Vegetation (FSVeg), U.S. Forest Service, United States Department of
279 Agriculture.
280 16. Ross, C.W., Loudermilk, E.L., O'Brien, J.J., Flanagan, S.A., McDaniel, J., Aubrey, D.P.,
281 Lowe, T., Hiers, J.K., Skowronski, N.S., 2024. Lidar-derived estimates of forest structure in
282 response to fire frequency. fire ecol 20, 44. https://doi.org/10.1186/s42408-024-00279-7
283 17. Roussel, J.-R., Auty, D., Coops, N.C., Tompalski, P., Goodbody, T.R.H., Meador, A.S.,
284 Bourdon, J.-F., De Boissieu, F., Achim, A., 2020. lidR: An R package for analysis of
285 Airborne Laser Scanning (ALS) data. Remote Sensing of Environment 251, 112061.
286 https://doi.org/10.1016/j.rse.2020.112061
287 18. Sumnall, M.J., Trlica, A., Carter, D.R., Cook, R.L., Schulte, M.L., Campoe, O.C., Rubilar,
288 R.A., Wynne, R.H., Thomas, V.A., 2021. Estimating the overstory and understory vertical
289 extents and their leaf area index in intensively managed loblolly pine (Pinus taeda L.)
290 plantations using airborne laser scanning. Remote Sensing of Environment 254, 112250.
291 https://doi.org/10.1016/j.rse.2020.112250

19. Texas Natural Resource Information System (TNRIS), 2018. Strategic Mapping Program (Stratmap). Upper Coast Lidar. Available at https://tnris.org/stratmap/elevation-lidar/ (Accessed on 15 October 2022)
20. Texas Water Development Board (TWDB), 2018. 2018 Coastal Texas Lidar Final QA/QC Report. Available at https://prd-tnm.s3.amazonaws.com/StagedProducts/Elevation/metadata/TX_CoastalRegion_2018_A18/TX_Coastal_B1_2018/reports/thrid-party-
21. United States Department of Agriculture (USDA), 2025. Secretary Rollins Announces Sweeping Reforms to Protect National Forests and Boost Domestic Timber Production [WWW Document], URL https://www.usda.gov/about-usda/news/press-releases/2025/04/04/secretary-rollins-announces-sweeping-reforms-protect-national-forests-and-boost-domestic-timber (accessed 4.29.25).
22. United States Department of Agriculture (USDA). Texas NAIP Imagery, 2018-12-31. Web. 2025-06-24.
23. van Aardt, J.A.N, 2000. Spectral Separability among Six Southern Tree Species (Master of Science in Forestry). Virginia Polytechnic Institute and State University, Blacksburg, VA.
24. Van Aardt, J.A.N., Wynne, R.H., 2007. Examining pine spectral separability using hyperspectral data from an airborne sensor: An extension of field-based results. International Journal of Remote Sensing 28, 431–436. https://doi.org/10.1080/01431160500444772
25. Woods, M., Lim, K., Treitz, P., 2008. Predicting forest stand variables from LiDAR data in the Great Lakes St. Lawrence forest of Ontario. The Forestry Chronicle 84, 827–839. https://doi.org/10.5558/tfc84827-6

26. Wu, J., Man, Q., Yang, X., Dong, P., Ma, X., Liu, C., Han, C., 2024. Fine Classification of Urban Tree Species Based on UAV-Based RGB Imagery and LiDAR Data. Forests 15, 390. https://doi.org/10.3390/f15020390